Activation Conditions Play a Key Role in the Activity of Zeolite CaY: NMR and Product Studies of Brønsted Acidity

Hsien-Ming Kao, Clare P. Grey,* Kasi Pitchumani, P. H. Lakshminarasimhan, and V. Ramamurthy*

Departments of Chemistry, State University of New York, Stony Brook, New York 11794-3400, and Tulane University, New Orleans, Louisiana 70118-5698

Received: December 2, 1997; In Final Form: February 5, 1998

CaY, activated under different conditions, was characterized with ^{1}H, ^{31}P, and ^{1}H/^{27}Al double resonance MAS NMR. The ^{1}H MAS NMR spectra of CaY, calcined in an oven at 500 °C, shows resonances from H_2O (bound to Ca^{2+} and the zeolite framework), $CaOH^+$, aluminum hydroxides, silanols, and Brønsted acid sites. No evidence for Lewis acidity is observed on adsorption of trimethylphosphine, and an estimate of ≈16 Brønsted acid sites per unit cell is obtained for this sample. CaY activated in an oven at higher temperatures contains less water, but all the other species are still present. In contrast, CaY activated by slow ramping of the temperature under vacuum to 500 or 600 °C shows a much lower concentration of Brønsted acid sites (<1/unit cell). Again, no evidence for Lewis acidity was observed. These NMR results have been utilized to understand the very different product distributions that are observed for reactions of 1,1- and 1,2-diarylethylenes in zeolite CaY activated in an oven (in air) and under vacuum. Samples with high concentrations of Brønsted acid sites react stoichiometrically with these sites, yielding diarylalkanes. At low concentrations, the Brønsted acid sites can act catalytically resulting in isomerization reactions.

Introduction

One of our groups has been investigating a number of reactions of unsaturated organic molecules inside the pores of zeolites such as X and Y.[1] In several of these studies involving divalent exchanged forms of the zeolites, the reactivities of the molecules were found to be very sensitive to the method of activation. For example, aryl olefins sorbed in activated CaY zeolites were observed to react to form the corresponding aryl alkanes, when CaY was activated in an oven. Very little reaction was observed for reactions using zeolites activated under a vacuum. These initial observations prompted a more detailed study of this phenomenon and the characterization of CaY activated under different conditions.

Divalent cation-exchanged zeolites have been previously studied with a variety of spectroscopy methods.[2−5] In this study, we extend the previous work on this, and similar zeolites, by carefully correlating the species that are present (e.g., $CaOH^+$, Brønsted acid sites) with the catalytic activity of the system. In particular, the dramatic differences between oven and vacuum activation are explored. 1,1- and 1,2-diarylethylenes are used as chemical probes of CaY activity, and variable-temperature ^{1}H MAS and ^{1}H/^{27}Al and ^{31}P/^{27}Al TRAPDOR NMR[6,7] are utilized to characterize the active sites (e.g., the Brønsted and Lewis acid sites) present in CaY. ^{1}H/^{27}Al and ^{31}P/^{27}Al TRAPDOR NMR methods are used to probe the H−Al and P−Al distances and are useful assigment tools.[6,7] Trimethylphosphine was sorbed on CaY, and ^{31}P/^{27}Al TRAPDOR NMR was used to probe Lewis acidity.

Dehydrated divalent cation-exchanged zeolites are known to act as catalysts for cracking and alkylation reactions, due to the acidic species formed by the dissociation of water.[8] Addition of a small amount of water to the dehydrated material has been observed to increase the activity, while a decrease in activity was observed with increased calcination temperatures. These observations could be rationalized by the formation, on adding water, of a number of Brønsted acid sites and MOH^+, where M represents an alkaline-earth divalent cation, followed by the subsequent recombination of the MOH^+ and acid sites to release water, on heating. Infrared studies of zeolite Y containing Ca^{2+} and Mg^{2+} and a small amount of adsorbed water have been reported.[2−4] An absorption band was observed at around 3600 cm^{-1} in dehydrated CaY, which increased significantly in intensity after readsorption of water, and was attributed to $CaOH^+$ groups.[3,4] X-ray diffraction has been performed to determine the distribution of Ca^{2+} cations on the different cation positions in a partially dehydrated sample of zeolite CaNaY (Si/Al = 2.37).[9,10] Ca^{2+} was located on site I′ and II, and H_2O on site II′. Recently, Hunger et al. have used ^{1}H MAS (magic angle spinning) NMR to study the mechanisms of the formation of hydroxyl groups in MgNaY and CaNaY.[5] On the basis of an empirical relation, obtained by Yesinowski et al.,[11] for the isotropic chemical shift of hydroxyl groups, versus the O−H···O bond lengths (where H···O respresents the hydrogen bond) they concluded that the resonances at 0.5 and 2.8 ppm observed in the ^{1}H MAS NMR spectrum of a CaNaY sample were due to $CaOH^+$ groups in the supercages and sodalite cages, respectively. In this report, we establish that CaY activated under air and under vacuum possess drastically different numbers of acidic sites and very different species; this is related to the catalytic properties.

Experimental Section

Preparation of CaY. NaY (Aldrich, 10 gm) was added to 200 mL of a 10% $Ca(NO_3)_2$ solution, and the slurry was stirred at 80 °C overnight. The slurry was filtered and the filtrate

* To whom correspondence should be addressed: C.P.G., State University of New York; V.R., Tulane University.

S1089-5639(98)00385-5 CCC: $15.00
Published on Web 04/22/1998

washed thoroughly with at least 2 L of distilled water. The above exchange procedure was repeated at least four times. The filtrate obtained after the wash was dried at room temperature in air. ICP analysis indicated that the zeolite thus obtained has a composition corresponding to $Si_{138.7}Al_{53.3}Na_{7.5}Ca_{23.3}O_{384}$.

Preparation of D_2O-Exchanged CaY. A known amount of CaY was stirred in D_2O at 60 °C for 6 h. The sample was filtered and once again stirred in D_2O at 60 °C. This process was repeated three times, and the final sample was stored under nitrogen. Activation was done under a nitrogen atmosphere.

Preparation of 1,1-Diarylethylenes (1, 4, and 7). 1,1-Diphenylethylene (**1a**) was purchased from Aldrich and used without further purification. All other olefins were prepared from the corresponding ketones by a Grignard reaction followed by a dehydration. The standard procedure adopted is described below: A 1 equiv amount of ketone was taken in dry diethyl ether solution under nitrogen atmosphere. To this, 1.5 equiv of methylmagnesium bromide (3 M solution in ether from Aldrich) was added, and the solution was stirred for another 1 h. The ether solution was then quenched with 0.1% aqueous HCl. The organic portion was extracted into ether and concentrated. The alcohol thus obtained was dehydrated by refluxing in 30 mL of benzene with a catalytic amount of *p*-toluenesulfonic acid. The product was purified by column chromatography by using petroleum ether/dichloromethane as the eluant. Required Grignard reagents for 1,1-diarylethylenes **4** and **7** were prepared from the corresponding ethyl bromide or isopropyl bromide, respectively.

Activation of Zeolites for the Product Studies. Two methods of activation were adopted: (A) in an oven under air; (B) on a vacuum line at a reduced pressure (5×10^{-4} Torr).

Method A: A known amount of zeolite was placed in a porcelain crucible in a preheated oven (100 to 700 °C) and activated under aerated conditions for approximately 10 hours.

Method B: A known amount of zeolite was placed in a quartz tube which was then attached to a vacuum line via Teflon fittings. The sample was degassed at room temperature for 3 h under reduced pressure (5×10^{-4} Torr) and then slowly heated (15 °C/5 min) under reduced pressure to the desired temperature (250−400 °C) and kept at that temperature for 10 h.

Inclusion of Olefins in Zeolites. The activated zeolite was cooled to room temperature and added to a hexane solution of the olefin (typically 20 mg of olefin for 300 mg of zeolite; hexane, 5 mL) and stirred for 3 h. The products were extracted from the zeolite by stirring the zeolite overnight with either dichloromethane or tetrahydrofuran. Products were analyzed by GC (Hewlett-Packard 5890; SE-30 capillary column). For identification purposes, the products were isolated by flash chromatography and characterized by NMR and GCMS.

Sample Preparation for NMR Experiments. Zeolite samples were dehydrated either in an oven or in a vacuum by slowly ramping the temperature to 500 or 600 °C over a period of 16 h. The samples were then held at this temperature for another 16 h. Some materials, prepared in the oven, were subsequently dehydrated at 110 °C overnight under vacuum to remove any residual weakly bound or physisorbed water. Trimethylphosphine (TMP, 99%, Alfa) was introduced into some samples at room temperature, over a vacuum line, to investigate the Brønsted and Lewis acidity. Details of the different sample preparations are given in Table 1. A sample of HY (Aldrich) (denoted TMP/HY-500-oven) was also activated and loaded with TMP, for comparison with the CaY studies. All samples were packed in a glovebox, under dry nitrogen, into MAS rotors for the NMR experiments.

TABLE 1: Different Samples Studied by NMR with the Activation Conditions, Loading Levels, and Nomenclature Used to Label the Samples Listed for the Different Samples

name	activation conditions	loading level
bare CaY	none	none
CaY-500-oven	500 °C in oven, 110 °C in a vacuum	none
CaY-600-oven[a]	600 °C in oven, 110 °C in a vacuum	none
CaY-500-vac	500 °C in a vacuum	none
CaY-200-vac[b]	200 °C in a vacuum	none
CaY-600-vac	600 °C in a vacuum	none
TMP/CaY-500-oven	500 °C in oven, 110 °C in a vacuum	33 TMP/uc (unit cell)
TMP/CaY-600-oven	600 °C in oven, 110 °C in a vacuum	24 TMP/uc
TMP/CaY-500-vac	500 °C in a vacuum	22 TMP/uc
TMP/CaY-600-vac	600 °C in a vacuum	19 TMP/uc
TMP/HY-500-oven	500 °C in oven, 110 °C in a vacuum	30 TMP/uc

[a] Sample was directly put into an oven held at 600 °C for 16 h. [b] Sample was calcined in a vacuum at 200 °C for 6 h.

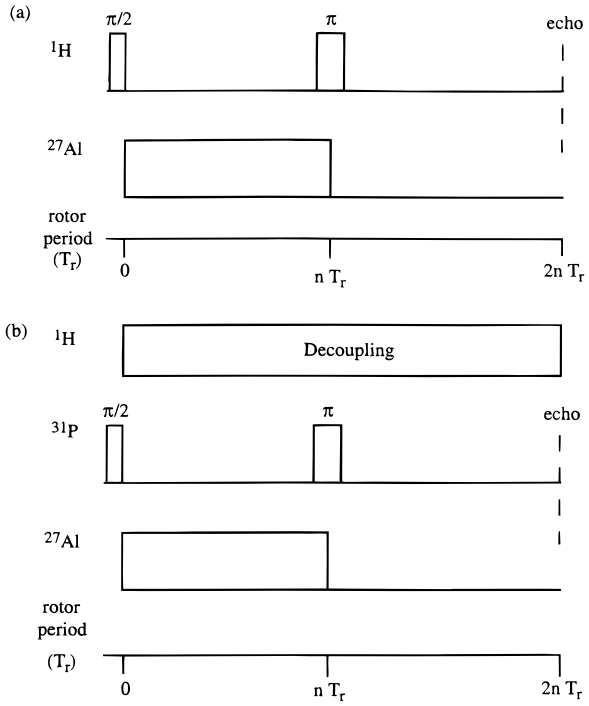

Figure 1. Pulse sequences used in the (a) ^{1}H/^{27}Al and (b) ^{31}P/^{27}Al TRAPDOR NMR experiments. The $\pi/2$ and π pulses are synchronized with the rotor period, in both (a) and (b). Intensities are measured from experiments performed with (I) and without ^{27}Al irradiation (I_0), the latter providing the control experiment.

NMR Experiments. NMR spectra were acquired on a Chemagnetics CMX-360 spectrometer with a triple-tuned Chemagnetics probe, tuned for ^{1}H (360 MHz), ^{31}P (142 MHz), and ^{27}Al (93 MHz). ^{1}H and ^{31}P $\pi/2$ pulse lengths of typically 5 and 6.5 μs and repetition times of 2 s were used. Chemical shifts for ^{31}P spectra are quoted relative to 85% H_3PO_4 as an external reference. An ^{27}Al rf amplitude (ν_1) of 55 kHz was used for the ^{1}H/^{27}Al and ^{31}P/^{27}Al TRAPDOR NMR experiments shown in Figure 1a,b. Refocusing at the rotor echo, of the $I = {}^1/_2$ nuclei (^{1}H or ^{31}P) that are coupled to quadrupolar nuclei S (^{27}Al), is prevented by the combination of magic angle spinning (MAS) and continuous irradiation of the S nuclei. This results in a loss of I-spin intensity at the spin−echo. More detailed theoretical descriptions of the TRAPDOR NMR experiment and some applications can be found in the refs 6, 7, and 12.

TABLE 2: Observations upon Inclusion of 1,1-Diphenylethylene within $M^{2+}Y$ Zeolites: Variation of Activation Conditions, Loading Level and Nature of Cation

condition[a]	diphenylethylene remaining (%)	product (%)[b,h] diphenylethane (**2**)	product (%)[b,h] benzophenone (**3**)	color[c]
		(a) Variation of Activation Conditions: CaY[d]		
CaY-100-oven	98		2	white
CaY-150-oven	95	4	1	light green
CaY-200-oven	69	30	1	light green
CaY-300-oven	15	74	1	green
CaY-400-oven	15	74	1	green
CaY-500-oven	5	85		green
CaY-600-oven	60	32		green
CaY-750-oven	96	4		light green
CaY-400-vacuum[e]	92	7		very light green
CaY-450-vacuum[e]	95	4		very light green
CaY-550-vacuum[e]	98	1		very light green
		(b) Variation of Loading Level: CaY-500-oven		
1 molecule/10 cages	1	78	1	green
1 molecule/4 cages	1	78	1	green
1 molecule/1 cage	5	74	1	green
1 molecule/0.5 cage	15	69	1	green
		(a) Variation of Cation: M^{2+}Y-500-Oven		
MgY	60	38	<1	
SrY	40	57	2	
BaY	99	1		
MgX; CaX; SrX; BaX[f]	99			
CaY/solid[g]	80		20	green

[a] The data presented here, except where it is stated to be "solid", correspond to a condition where the mixing was done in a hexane slurry. [b] The yield corresponds to the amount found in the reacted material. Yield is based on GC analysis in the presence of an internal standard. Isolated yield varied between 80 and 95%. [c] The color of the slurry after addition of diphenylethylene to the activated zeolite. [d] The amount of diphenylethylene was maintained at one molecule per two supercages. [e] The sample was activated on a vacuum line at 10^{-4} Torr. [f] None of the $M^{2+}X$ zeolites showed behavior similar to that of $M^{2+}Y$. [g] The solid zeolite and diphenylethylene were ground on a mortor and left in a vial. The green color appeared immediately upon mixing. [h] The yields of dimeric alkene and an indenyl product are not provided.

TABLE 3: Obervations upon Inclusion of 1,1-Diarylethylenes within $M^{2+}Y$ Zeolites: Generality of the Phenomenon

	olefin remaining (%)	product (%)[b] diphenylethane (**2**)	product (%)[b] benzophenone (**3**/**6**)	color[c]	diffuse reflectance max (nm)
p,*p*'-dimethoxy DPE (**1b**)	78	21	1	bright orange	486 (strong), 680 (weak)
p-methoxy DPE (**1c**)	39	57	4	cream	452 (strong), 653 (weak)
p,*p*'-dimethyl (**1d**)	68	24	7	bright yellow	457 (strong), 642 (very weak)
p,*p*'-dichloro (**1e**)	95	2	3	greenish yellow	462 (strong), 630 (weak)
p,*p*'-difluoro (**1f**)	95	1	4	cream	436 (weak), 610 (weak)
1,1-diphenyl-1-propene (**4a**)	48	20	32 (**6a**)	orange	444
1,1-bis(*p*-methoxyphenyl-1-propene (**4b**)	77	5	18 (**6b**)	bright orange	496
1,1-diphenyl-2-methyl 1-propene (**7a**)	98	2		orange	454
1,1-bis(*p*-methoxyphenyl)-2-methyl-1-propene (**7b**)	95	4		bright orange	498

Diffuse Reflectance Spectra. DR spectra were recorded by packing the sample in a 1 mm quartz cell. The background correction was done by recording a spectrum of $BaSO_4$ in the same cell. The recorded spectrum for the sample was converted into Kubelka Munk by the program supplied with the instrument (Shimadzu model 2101 PC).

Results

Product Studies. Two sets of olefins were used as probes to examine the reactivity of CaY. The first set of olefins are the 1,1-diarylethylenes (**1a**−**f**), and the second set are the 1,2-diarylethylenes (**9a**−**d** and **11a**−**d**). The substituents are present in the *para*-position of the aryl ring in both cases. CaY was activated by using two different methods. In the first, designated as CaY-temp-oven, the zeolite was activated in air in an oven at a specified temperature (between 100 and 750 °C). For example, CaY-500-oven refers to a sample that was activated at 500 °C in an oven. In the second method, designated as CaY-temp-vacuum, the zeolite was activated on a vacuum line at temperatures between 400 and 550 °C. The majority of the experiments were carried out with the sample CaY-500-oven.

When CaY-500-oven was added to a hexane solution of 1,1-diphenylethylene, the zeolite−hexane slurry turned yellow and then green and remained green for several days. This phenomenon was general to all the diarylethylenes **1b**−**f**, and a variety of brightly colored zeolitic samples were produced. The products were extracted from these samples with either dichloromethane or tetrahydrofuran and were identified by their NMR and mass spectral characteristics. Diarylethanes **(2a**−**f)** were the major products isolated, along with small amounts of the corresponding diaryl ketones (Tables 2 and 3; Scheme 1), and the zeolite was left with a blue color which persisted for at least 10 days. Extraction of the zeolite upon acid treatment results in two additional products: adimeric alkene and an indenyl product. Substituents on the aryl groups resulted in reduced conversions, the smallest conversions being observed for the difluoro (**1f**) and dichloro (**1e**) compounds.

The reactivity of diarylethylenes in CaY was very sensitive to the method used to activate CaY (Table 2). The reaction

SCHEME 1: Products upon Inclusion of Diarylethylenes within Activated CaY

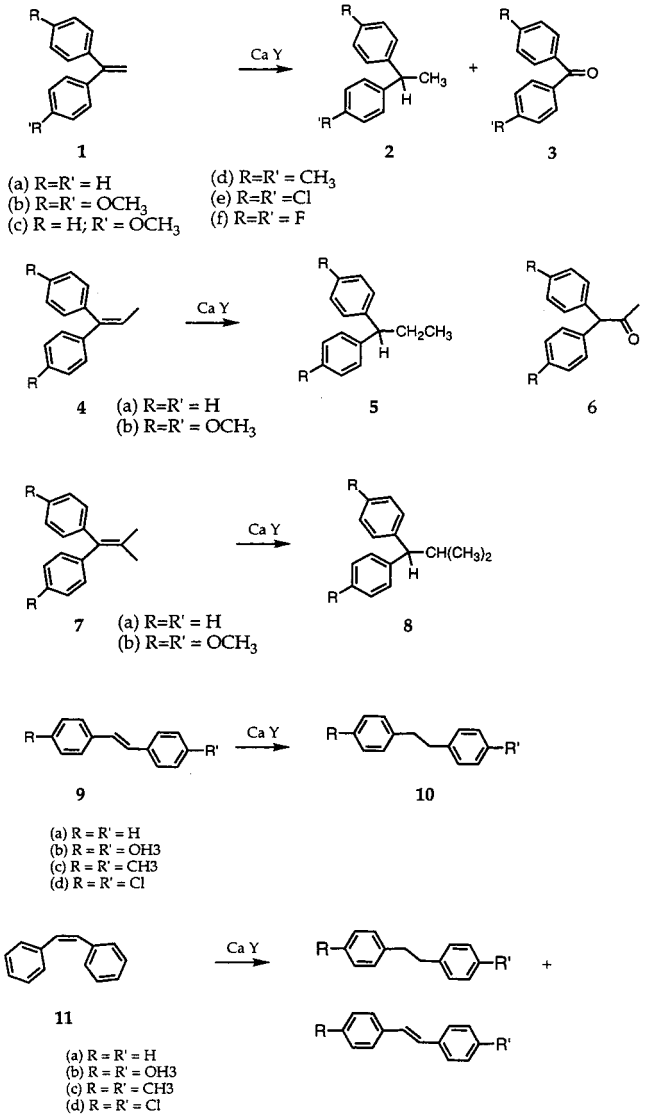

was nearly quantitative toward reduction of **1a** when the sample CaY-500-oven was used (Table 2a). Surprisingly, reactions performed with CaY-750-oven and CaY-400-vacuum showed very little activity: When these zeolites were added to **1a**, no bright coloration was observed; nor was a significant amount of the reduced product **2** formed. CaY was least active when it was activated in an air oven below 150 °C or when it was activated on a vacuum line above 400 °C. Low activity of the former sample is most likely due to the presence of residual water which prohibits the entry of an olefin into the zeolite. The effect of the loading level of **1a** in CaY-500-oven on the reactivity was also explored (Table 2b). Little difference in the percent of diarylethane formation was observed at low loading levels. A slight reduction in product formation was observed when the loading level was increased from 1 molecule in 4 supercages to 1 molecule per cage.

The reactivity of **1a** in a series of divalent cation exchanged X and Y zeolites was also explored (Table 2c), and the activity was observed to decrease in the order Ca > Sr > Mg > Ba for the Y series. Negligible activity was observed in the X series in comparison to the Y series, BaY showing behavior similar to those of X zeolites.

Similar to reactions of **1**, olefins **9a**−**d** and **11a**−**d** were reduced to the corresponding 1,2-diarylethanes (**10**) in CaY-500-oven (Scheme 1). Again, consistent with the observations made for the 1,1-diarylethylenes, addition of CaY-450-vacuum to *trans*-1,2-diarylethylenes **9a**−**d**, resulted in no observable reaction. Surprisingly, *cis*-1,2-diarylethylenes **11a**−**d** were quantitatively isomerized to the trans isomer **9a**−**d**, in CaY-450-vacuum, without any reduction taking place.

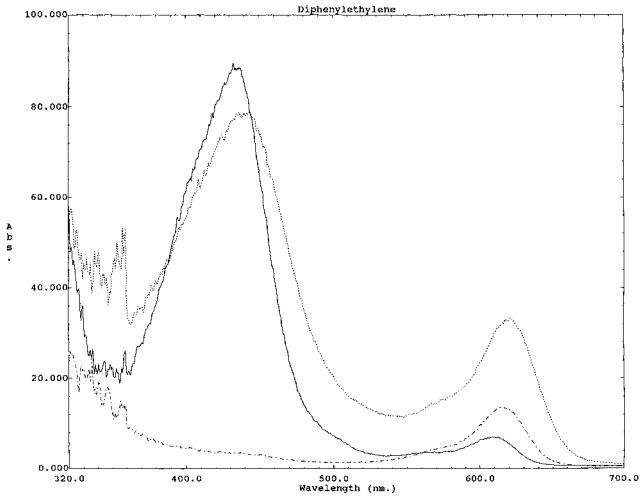

Figure 2. Diffuse reflectance spectra of diphenylethylene and 1,1-diphenyl ethane-1-ol included within activated CaY-500-oven: diphenylethanol (continuous line); diphenylethylene (dashed line); diphenylethylene after washing with methylene chloride (broken line).

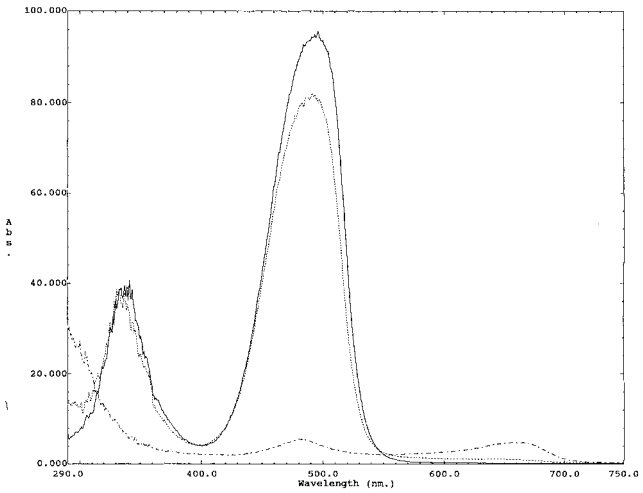

Figure 3. Diffuse reflectance spectra of 1,1-bis(4-methoxyphenyl)-ethylene and 1,1-bis(4-methoxyphenyl)ethan-1-ol in CaY-500-oven: 2,2-bis(*p*-methoxyphenyl)ethanol (continuous line); 1,1-bis(4-methoxyphenyl)ethylene (dashed line); 1,1-bis(4-methoxyphenyl)ethylene in CaY after washing with methylene chloride (broken line).

Characterization of Reactive Intermediates by Diffuse Reflectance Spectroscopy. Diffuse reflectance spectra were acquired in order to study the cause of the deep colors formed on addition of the diarylethylenes. The diffuse reflectance spectra displayed in Figures 2 and 3, for 1,1-diphenylethylene **(1a)** and 1,1-bis(4-methoxyphenyl)ethylene **(1b)**, respectively, consist of two distinct maxima (one below 500 nm and the other above 600 nm). Following extraction of the products from the zeolite with either diethyl ether or tetrahydrofuran, which changes the color of the zeolite from green to blue, the spectra consist mainly of the absorption above 600 nm. This suggested that two independent species are responsible for the two absorptions. One possible assignment of the intermediate responsible for the shorter wavelength absorption (428 nm for 1,1-diphenylethylene and 486 nm for 1,1-bis(4-methoxyphenyl)-

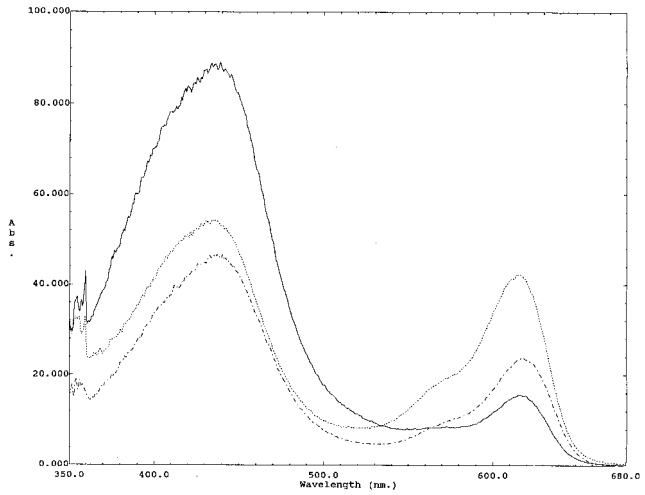

Figure 4. Time-dependent diffuse reflectance spectra of diphenylethylene in CaY-500-oven. Note the development of the peak at 618 nm with time: (continuous line) within 15 min of addition; (dashed line) 20 h after addition; (broken line) 40 h after addition.

SCHEME 2: Brønsted Acid-Site-Mediated Reduction of Diarylethylenes

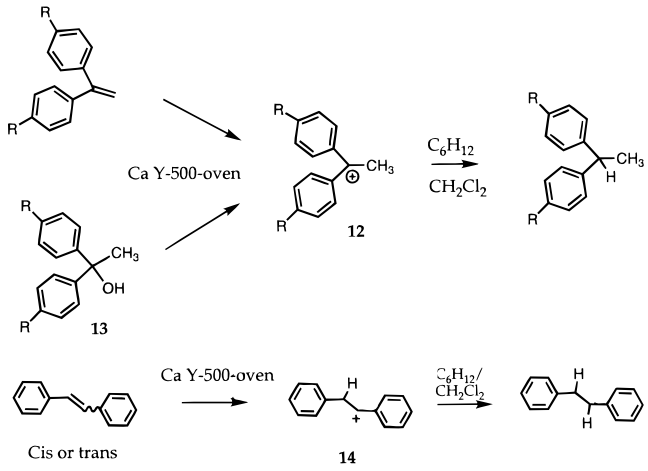

ethylene), based on literature reports,[13] is the carbocation **12**, derived via the protonation of the parent olefin (Scheme 2). This was confirmed by generating the same carbocations (**12**) independently from the corresponding carbinols **13** (Scheme 2). The spectra from 1,1-diphenyl ethan-1-ol and 1,1-bis(4-methoxyphenyl)ethan-1-ol sorbed in CaY are shown in Figures 2 and 3, respectively, and are nearly identical at short wavelengths.

The time-dependent diffuse reflectance spectra show changes in the relative intensities of the two absorptions as a function of time (Figure 4). The absorption assigned to the monomer-cation **12** dominates the time-dependent diffuse reflectance spectra of diphenylethylene in CaY-500-oven (Figure 4) at early times, but with time, the second absorption at 618 nm grows in at the expense of the monomer-cation peak. The identity of the species responsible for this absorption is discussed in a later section.

The diffuse reflectance spectra of the 1,2-diarylethylenes (**9** and **11**) in CaY showed absorptions in the region 300−370 nm, and no longer wavelength absorptions were present. The absorption in the region 300−370 nm is attributed to a benzyl carbocation derived by the addition of a proton to **9** and **11**.[14] Inclusion of **4** and **7** (Scheme 1) within CaY-500-oven gave a bright orange color (Table 3). The diffuse reflectance spectrum of this yellow solid consisted of a single absorption as shown in Figure 5.

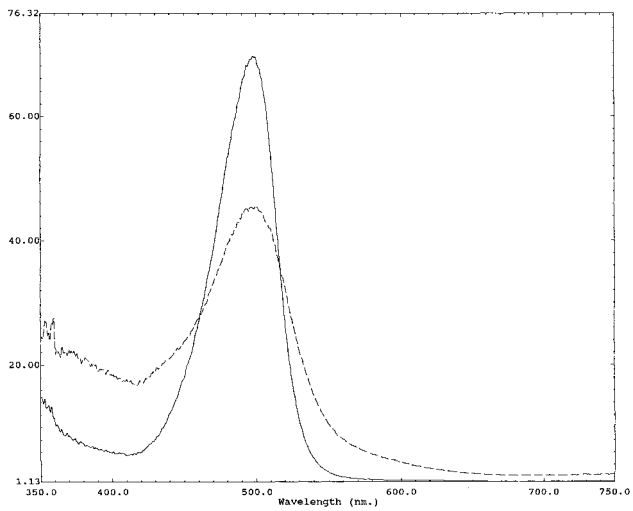

Figure 5. Diffuse reflectance spectra of 1,1-bis(4-methoxyphenyl)-prop-1-ene (**4b**) (continuous line) and 2-methyl-1,1-bis(4-methoxyphenyl)prop-1-ene (**7b**) (dashed line) in CaY-500-oven.

Isotope Studies of the Reaction Mechanism. The major product upon inclusion of 1,1-diarylethylenes (**1a**−**f**) and 1,2-diarylethylenes (**9a**−**d** and **11a**−**d**) within CaY results from the addition of two hydrogen atoms to the π-bond. One possibility for the first step in the reduction process involves the addition of a proton to the olefin (Scheme 2). This suggestion is consistent with the diffuse reflectance measurements, where the carbocation was observed as a stable intermediate. To test this, and other possible reaction mechanisms, reactions were performed with CaY that had previously been washed with D_2O and CaY(D_2O) to remove the H_2O and to deuterate any water or hydroxyl groups that remain following activation. Sorption and reaction studies were performed in deuterated solvents, and the products were analyzed with mass spectroscopy to determine the level and positions of any deuterium incorporation in the products. Results from these studies were contrasted with those obtained with CaY(H_2O) in deuterated solvents (C_6D_{12} and CD_2Cl_2) and are shown in Scheme 3.

Figure 6a shows the mass spectral fragmentation pattern for diphenylethane obtained in a deuterated solvent after extraction, when nondeuterated CaY(H_2O) was used. The mass ion at *m*/*e* 182 and the base peak at *m*/*e* 167, due to CH_3 loss, are clearly seen, consistent with presence of 1,1-diphenylethane with a "D" in carbon-1. In contrast, when CaY(D_2O) was used, a mass ion at *m*/*e* 183, and a base peak at *m*/*e* 168 (Figure 6b) were observed, which result from 1,1-diphenylethane in which the carbon-2 was substituted with a "D" instead of an "H". This is consistent with the suggestion that the initial protonation occurs at the carbon-2 of diphenylethylene and that the proton comes from acid sites present in CaY via the included H_2O or D_2O.

Characterization of CaY by NMR: Quantification of Acidic Sites. *CaY-500-oven.* Figure 7 shows the variable-temperature ^{1}H MAS NMR of a CaY sample (CaY-500-oven) calcined in an oven at 500 °C. Only one major resonance at 3.7 ppm, with small spinning sidebands and a shoulder at 4.5 ppm, is observed at room temperature. The former observation suggests that this resonance results from a number of species in rapid exchange with each other. Very low intensity spinning sideband manifolds, which spread over more than 100 ppm, are also visible when the spectrum is enlarged. These are assigned to water rigidly held to the zeolite lattice. On cooling of the sample, more resonances become visible as the exchange process between water and the other species starts to freeze out. At −150 °C, three major resonances at 3.7, 2.4, and 1.2 ppm

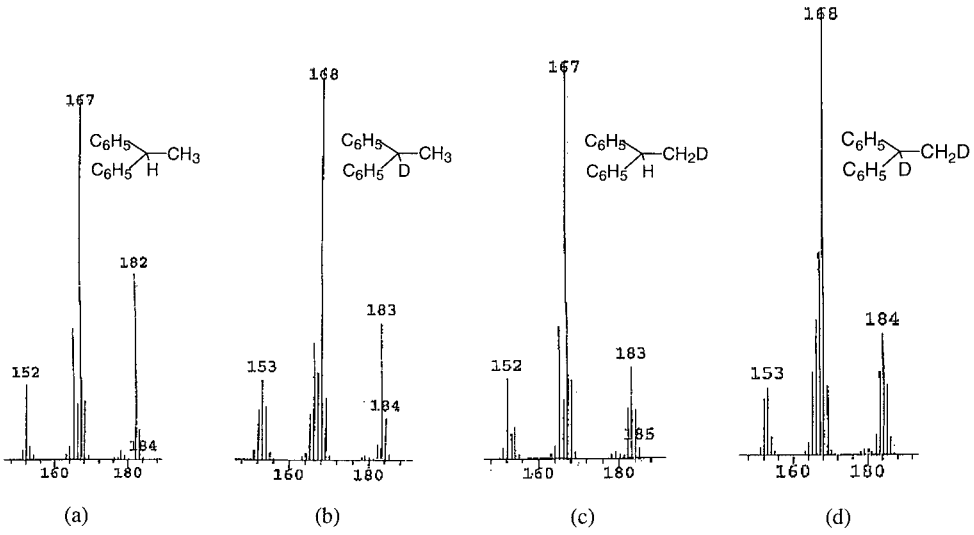

Figure 6. Mass spectra of the four H/D isomers of diphenylethane. See Scheme 3 for details.

SCHEME 3: Possible Sources of Hydrogens during the Conversion of Diarylethylenes to Diarylethanes

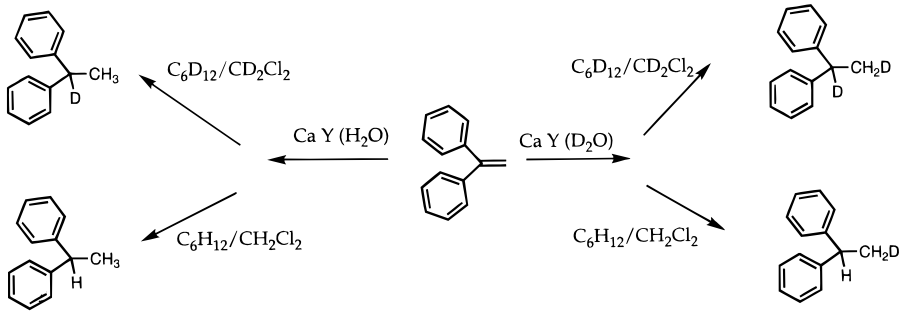

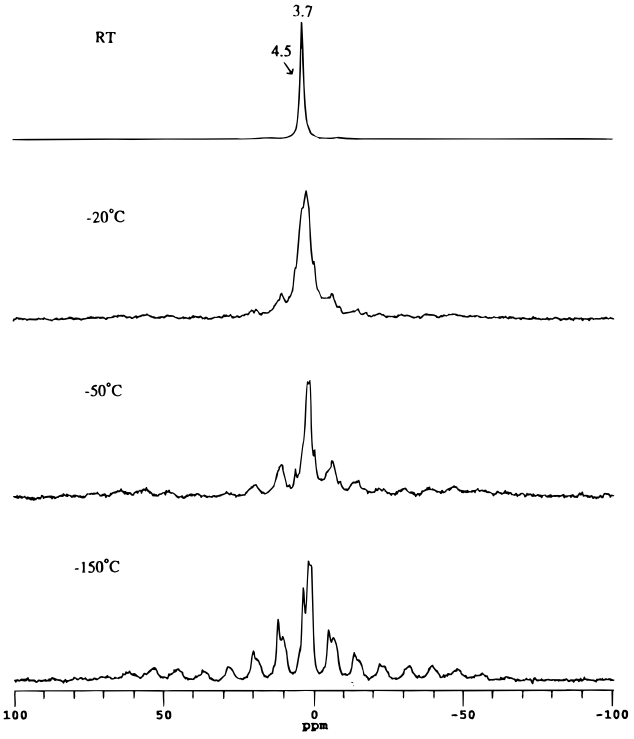

Figure 7. Variable-temperature ^{1}H MAS NMR spectra of CaY-500-oven collected at a spinning speed of 3 kHz.

and a shoulder at approximately 5 ppm are observed. The resonances at 3.7, 5.0 and 2.4 ppm are assigned to the Brønsted acid sites (3.7 and 5.0 ppm) and Al−OH groups (2.4 ppm). Spinning sidebands with an envelope resembling a "Pake doublet" (due to two isolated, strongly coupled ^{1}H spins) are also observed; this is consistent with the sideband pattern expected for two protons in a rigidly bound water molecule, the sidebands resulting from the proton−proton dipolar coupling between the two protons. This resonance, which has an isotropic chemical shift close to that of the Brønsted acid sites, is tentatively assigned to water bound to a calcium cation, i.e., $Ca(OH_2)_n^{2+}$ ($n = 1$).

^{1}H/^{27}Al TRAPDOR NMR experiments have been performed on this sample as shown in Figure 8. The intensities of the resonances of proton species that are nearby aluminum atoms are expected to decrease in the spectrum acquired with ^{27}Al irradiation. This occurs because the dephasing during the evolution time of the spin−echo experiment, due to ^{1}H−^{27}Al dipolar coupling, is no longer refocused on applying ^{27}Al irradiation.[12] Thus, the only proton species observed in the difference experiment are those that are nearby to aluminum atoms. As expected, the Brønsted acid sites (3.7 ppm) and Al−OH groups (2.4 ppm) show large ^{1}H/^{27}Al TRAPDOR effects in the difference spectrum (Figure 8c). Two resonances at 2.1 and 1.2 ppm, with weak and significantly more intense spinning sidebands, respectively, are observed in the spectrum obtained with ^{27}Al on-resonance irradiation (Figure 8b), implying that that these two species are not in close proximity to aluminum atoms. Two different $CaOH^+$ groups that resonate at 0.5 and 2.8 ppm have been reported previously and have been assigned to groups located in the supercages and sodalite cages, respectively.[5] Unfortunately, these resonances are very close in chemical shift to those of Al−OH and Si−OH species and it is difficult to assign these groups unambiguously. Neither of the species that resonate at 2.1 ppm or at 1.2 ppm can be

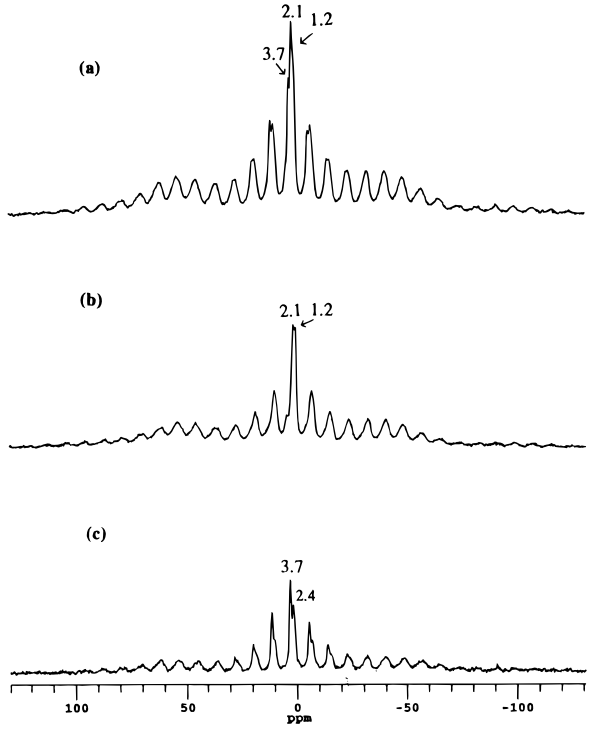

Figure 8. $^{1}H/^{27}Al$ TRAPDOR spectra of CaY-500-oven at −150 °C obtained (a) without and (b) with on-resonance ^{27}Al irradiation during τ (τ = 333 μs, spinning speed = 3 kHz). The difference spectrum is shown in (c). The intensity of (c) has been scaled by a factor of 2 with respect to (a) and (b).

assigned to Al−OH groups, however, since they are observed in the double resonance experiment (Figure 8b), and the TRAPDOR fractions ($1 - I/I_0$), where I_0 and I represent the ^{1}H echo intensities obtained without and with ^{27}Al irradiation, respectively, for these species are expected to be close to 1.0, under conditions used in our experiments.[6] On the basis of this, and the chemical shift, we tentatively assign the resonance at 2.1 ppm to a $CaOH^+$ and the resonance at 1.2 ppm to a silanol group. A significant $^{1}H/^{27}Al$ TRAPDOR effect was seen for the Pake doublet (Figure 8c) indicating that the water molecules are in close proximity to aluminum atoms.

TMP/CaY-500-oven. The variable-temperature ^{31}P proton-decoupled MAS NMR spectra of the sample TMP/CaY-500-oven are shown in Figure 9. Two broad resonances at −4 and −61 ppm were observed at room temperature. As the temperature decreases, the resonance at −4 ppm shifts to higher frequency and grows in intensity. Small spinning sidebands are observed at −100 °C and below. In contrast, the resonance at −61 ppm initially shifts slightly and sharpens (−20 °C). At lower temperatures, other smaller resonances become visible, and at −150 °C, the major resonance has shifted to −66 ppm and has two shoulders at −56 and −61 ppm. The resonance at −2 ppm has been assigned to a $TMPH^+$ species, resulting from the reaction of TMP and the Brønsted acid sites, and the resonance at −66.0 ppm was assigned to liquidlike TMP species.[15,16] TMP bound to an aluminum Lewis acid sites is expected to resonate in the range of −46 to −50 ppm,[7] and the absence of a resonance in this range suggests that there are no accessible Lewis acid sites for TMP. $^{31}P/^{27}Al$ TRAPDOR NMR experiments were performed, to confirm that the additional resonances are not in fact due to TMP binding to aluminum Lewis acid sites (Figure 10). As seen in the difference spectrum (Figure 10c), only the resonance at −2 ppm assigned to $TMPH^+$ shows a significant loss of intensity on ^{27}Al irradiation.

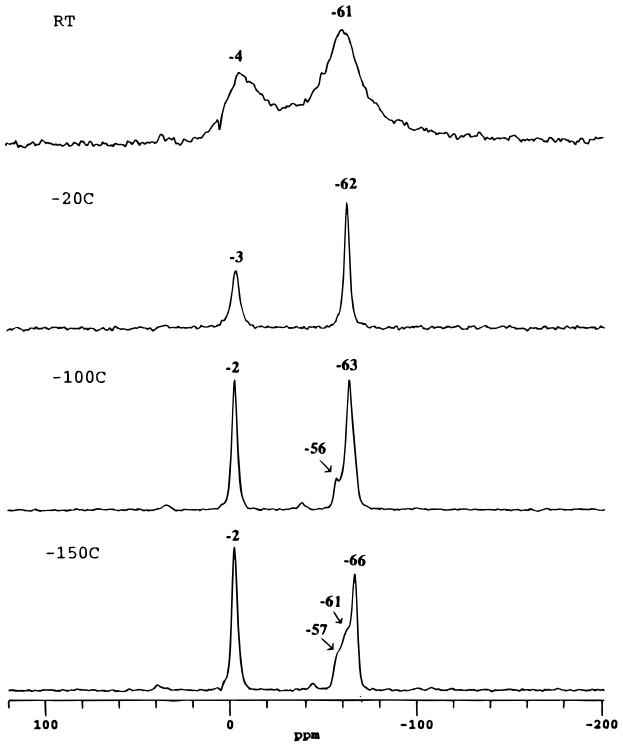

Figure 9. Variable-temperature ^{31}P $\{^{1}H\}$ MAS NMR spectra of TMP/CaY-500-oven collected at a spinning speed of 5260 Hz.

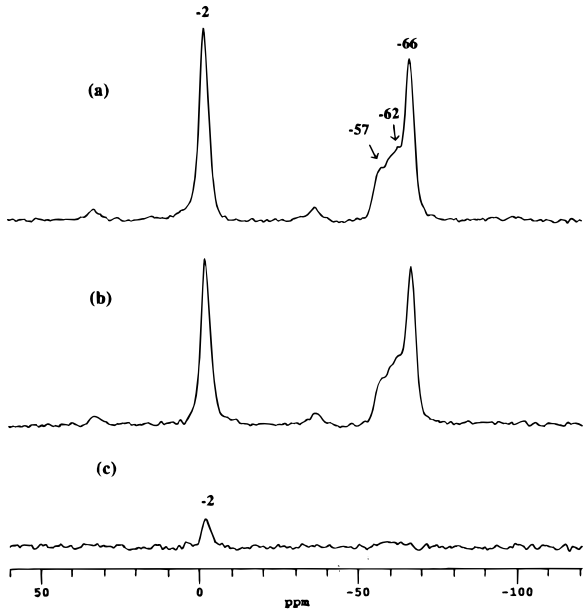

Figure 10. $^{31}P/^{27}Al$ TRAPDOR NMR spectra of TMP/CaY-500-oven obtained (a) without (b) with on-resonance ^{27}Al irradiation. The difference spectrum is shown in (c). (spinning speed = 5040 Hz; ^{27}Al rf field = 55 kHz; ^{27}Al irradiation time = 398 ms).

CaY-600-oven. Figure 11 shows the room-temperature $^{1}H/^{27}Al$ TRAPDOR spectra of a sample CaY-600-oven that was calcined in oven at 600 °C directly without any ramping period. The concentration of water in this sample has diminished considerably, as seen by the existence of significant spinning sideband manifolds, even at room temperature. Three major resonances at 3.4, 2.8, and 1.2 ppm were observed in the control experiment (Figure 11a). Three resonances were seen at 3.4, 2.4, and 0.8 ppm, with a shoulder at 3.7 ppm, in the difference spectrum (Figure 11c) indicating that these resonances arise from species near aluminum atoms. Both the resonances at 3.4 (with

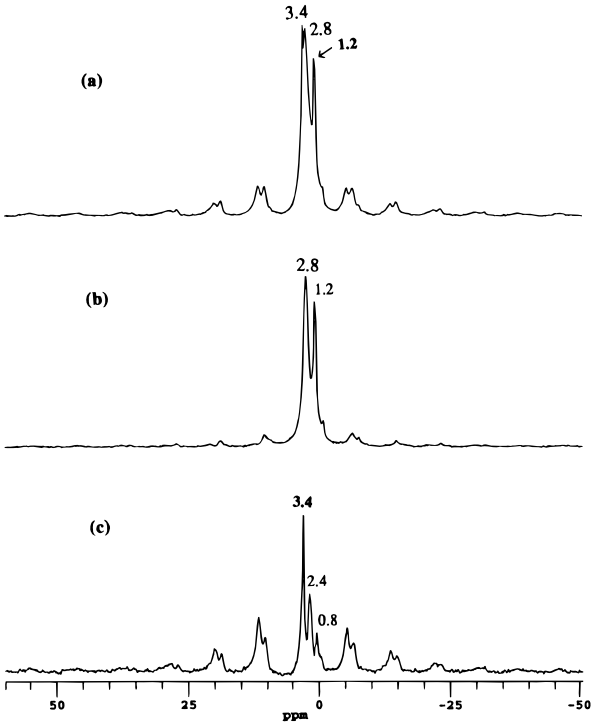

Figure 11. $^{1}H/^{27}Al$ TRAPDOR NMR spectra of CaY-600-oven obtained (a) without (b) with ^{27}Al on-resonance irradiation. The difference spectrum is shown in (c) (spinning speed = 3 kHz; ^{27}Al rf field = 55 kHz; ^{27}Al irradiation time = 333 ms).

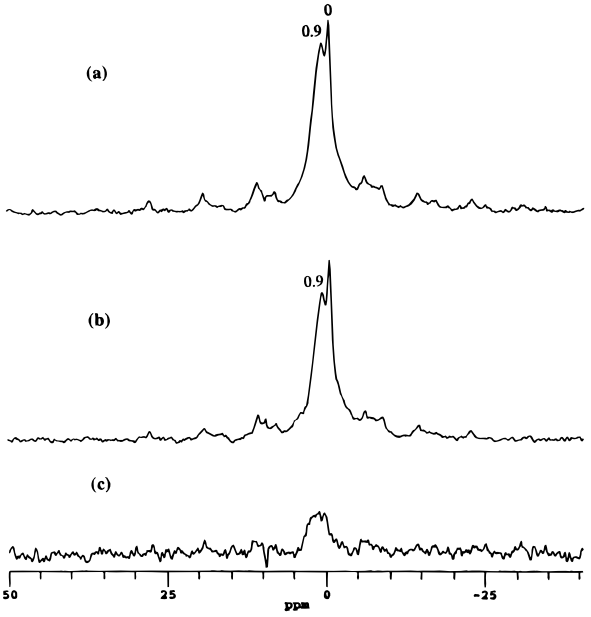

Figure 12. $^{1}H/^{27}Al$ TRAPDOR NMR spectra of CaY-500-vac obtained (a) without (b) with ^{27}Al on resonance irradiation. The difference spectrum is shown in (c) (spinning speed = 3 kHz; ^{27}Al rf field = 55 kHz; ^{27}Al irradiation time = 333 μs).

a shoulder at 3.7 ppm) and 2.4 ppm have large spinning sideband manifolds which are similar to those expected for Al−OH groups, and these resonances are assigned to Brønsted acid protons and Al_{tel}−OH, respectively, based on our earlier studies of dehydroxylated HY.[6] The resonance due to Al_{tel}−OH is clearly obscured in the control experiment, by the larger resonance at 2.8 ppm. The resonance at 0.8 ppm is assigned to Al_{oct}−OH groups, again on the basis of previous studies.[6] The spectrum obtained with ^{27}Al irradiation (Figure 11b) shows two major resonances at 2.8 and 1.2 ppm. The resonance at 2.8 ppm is associated with larger spinning sideband manifolds than the resonance at 1.2 ppm; this is more clearly visible when the spectrum is enlarged. This observation is similar to that made for the resonances at 2.1 and 1.2 ppm in the spectrum of CaY-500-oven acquired under similar conditions (Figure 8b), and the resonance at 2.8 ppm is tentatively assigned to a $CaOH^+$ group. Again, the resonance at 1.2 ppm is due to a silanol group. Interestingly, the resonance at 3.4 ppm comprises broader and sharper overlapping resonances, and the sideband manifolds appear to be coming from the broader component. The broader and sharper components are assigned to isolated Brønsted acid sites and Brønsted acid sites that are undergoing an exchange process with water molecules in the sample, respectively.

TMP/HY-500-oven. To compare the effect of oven versus vacuum activation, HY was also activated at 500 °C. The ^{31}P spectrum shows an intense resonance at −2 ppm that is assigned to $TMPH^+$. This resonance is now considerably more intense than the resonances in the range of −56 to −66 ppm, consistent with the increased number of Brønsted acid sites in this sample. Again, there are no resonances at around −46 ppm from TMP bound to the aluminum Lewis acid sites.

TMP/CaY-500-vac. The resonance at −60 ppm, resulting from physisorbed TMP, dominates in the ^{31}P spectra of TMP/CaY-500-vac and TMP/CaY-600-vac (not shown), and no detectable concentration of $TMPH^+$ is observed. On the basis of our earlier study of TMP adsorption in activated NaY zeolites, we estimate that we are sensitive to levels of ≈1 Brønsted acid site per unit cell with this method,[17] and hence, less than these detectable levels are present in these samples. Again, no resonances that can be assigned to TMP bound to the aluminum Lewis acid sites were detected. Figure 12 shows the room-temperature $^{1}H/^{27}Al$ TRAPDOR NMR spectra of CaY-500-vac. Only a negligible concentration of Brønsted acid sites (at around 4 ppm) was observed. The resonance at 0.9 ppm dominates the spectra, the resonance at around 0.0 ppm being caused by the probe head background. Similar spectra were observed for CaY-600-vac except that even lower concentrations of Brønsted acid sites were observed. The resonance at 0.9 ppm does not show a significant TRAPDOR effect on ^{27}Al irradiation (Figure 12b). Instead, a broad resonance in the range of 0.7−2.6 ppm was observed in the difference spectrum of $^{1}H/^{27}Al$ TRAPDOR NMR experiment (Figure 12c). Since the observed TRAPDOR effect for the resonance at 0.9 ppm is much less than that expected for Al−OH groups, this suggests that this resonance is due to $CaOH^+$ groups possibly in the supercages.

^{27}Al MAS NMR of the dehydrated samples shows a small resonance at 80 ppm that is assigned to the tetrahedral aluminum oxide anion in the sodalite cage[18] and is approximately 3−5% of the intensity of the resonance from the framework aluminum atoms.

CaY-200-vac. The $^{1}H/^{27}Al$ TRAPDOR NMR spectra of CaY-200-vac are shown in Figure 13. Two major resonances were observed at 2.1 and 3.7 ppm with shoulders at 5.0, 1.2, and 0.7 ppm. As described above, the resonances at 2.1, 1.2, and 3.7 ppm are tentatively assigned to $CaOH^+$ groups in the sodalite cages, silanol groups, and Brønsted acid sites, respectively. As shown in Figure 13b, resonances at 5.5, 2.1, and 1.2 ppm with a shoulder at 0.7 ppm were observed when ^{27}Al irradiation was applied. Resonances at 3.7, 2.4, and 0.8 ppm show significant TRAPDOR effects (Figure 13c). The latter two species were assigned to extraframework Al−OH groups. Therefore, the resonance at 0.7 ppm can be assigned to a $CaOH^+$ group in the supercages, consistent with the observation for the CaY-500

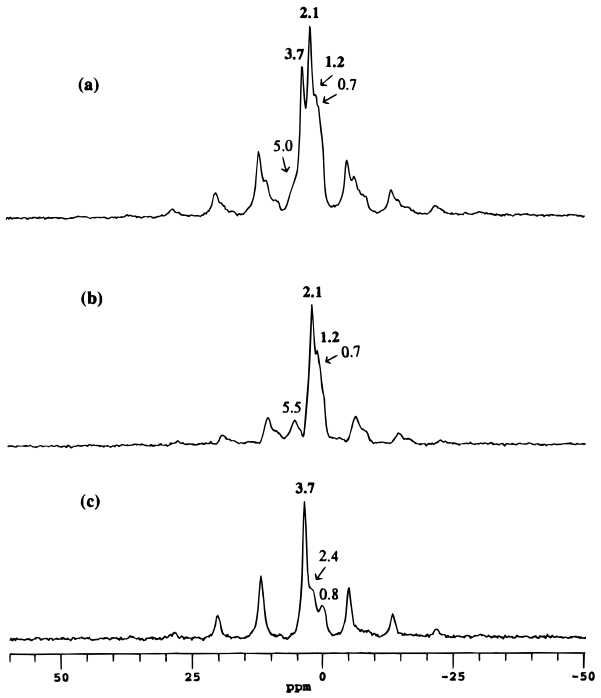

Figure 13. $^{1}H/^{27}Al$ TRAPDOR NMR spectra of CaY-200-vac obtained (a) without (b) with ^{27}Al on-resonance irradiation. The difference spectrum is shown in (c) (spinning speed = 3 kHz; ^{27}Al rf field = 55 kHz; ^{27}Al irradiation time = 333 μs).

(or 600)-vac sample and is close to the result reported by Hunger et al.[5] No TRAPDOR effect was observed for the resonance at 5.5 ppm indicating that it is probably due to mobile water molecules.

Discussion

The MAS NMR results are discussed first. This is followed by a discussion of the chemical behavior of CaY toward diaryl olefins. The diaryl olefin reactions and reactivity of CaY are interpreted by making use of the MAS NMR results and the different species detected with this technique.

Partly on the basis of earlier assignment of the resonances at 0.5 and 2.8 ppm in a sample of CaY to two different $CaOH^+$ groups located in the supercages and sodalite cages, respectively,[5] we assigned ^{1}H MAS NMR resonances observed at 2.1−2.8 ppm in this study to $CaOH^+$ ions present in the sodalite cages. The intensity of the resonance at 2.1 ppm was also observed to vary significantly from sample to sample, indicating that the presence of the species resonating at 2.1 ppm is very sensitive to the activation conditions, as expected. The shift from 2.8 ppm (CaY-600-oven, spectrum collected at room temperature) to 2.1 ppm (CaY-500-oven, spectrum collected at −150 °C) of the $CaOH^+$ resonance suggests that the isotropic chemical shift of this group may depend on both the water content and the temperature of the sample. The larger sideband manifolds associated with these resonances, in comparison to those of the silanol groups, probably result from dipolar coupling to nearby water molecules; residual water is more likely to be closer to the $CaOH^+$ group than to the silanol group and may be present as $Ca(H_2O)(OH^+)$, consistent with the assignment. The water in the $Ca(H_2O)(OH)^+$ species is likely to be in exchange with other $Ca(OH)^+(H_2O)_n$ groups in the same cage, especially at higher water contents. This may account for the changes in chemical shift with sample activation temperature and the temperature of the NMR experiment. X-ray diffraction data showed that the population of Ca^{2+} cations per cavity is less in the supercage (site II) in comparison to the sodalite cage (site I′) decreasing for higher water. For example, the populations per unit cell vary from 10.6−6.6 at site II and 12.0−17.3 at site I′ for samples with 12.8−26.5 water molecules per unit cell.[9,10] Thus, in the oven-activated samples that contain considerable amounts of water, the concentrations of $CaOH^+$ are expected to be extremely low, and the intensity due to the $CaOH^+$ groups in sodalite cages will be larger than that for the $CaOH^+$ groups in supercages. This is consistent with the experimental observations, where a resonance at 0.5−0.9 ppm from the $CaOH^+$ in the supercages was not observed in the ^{1}H MAS NMR of these samples. Since the intensity from this species is expected to be extremely small, the resonance may be obscured by the Al_{oct}−OH species at 0.8 ppm. The $CaOH^+$ supercage resonance is observed, however, in samples activated in a vacuum where the populations of site II calcium cations are known to be larger. A resonance was also seen (at 0.7 ppm) for oven activation at 200 °C, which was assigned to the $CaOH^+$ supercage groups. Possibly, a larger fraction of the calcium ions is present as $CaOH^+$ for activation at these lower temperatures.

A significant $^{1}H/^{27}Al$ TRAPDOR effect was seen for the water molecules (Figure 8) assigned to $Ca(OH_2)_n^{2+}$. This suggests that the water is also hydrogen bonded to oxygen atoms that are directly bound to aluminum atoms. This is possible in the sodalite cage, where water molecules can be simultaneously coordinated to calcium cations in site I′ and to the zeolitic framework occupying sites such as site II′. Indeed, calcium occupation of site I′ has been suggested to occur only when a small amount of residual water holds the cations in these sites (as opposed to site I).[19] The possibility of the coordination between water and Lewis acid sites (in the supercages) was excluded because significant concentrations of Lewis acid sites were not detected when TMP was used as a probe molecule (see below). However, it is possible that some of the TRAPDOR effect is caused by water molecules coordinated to both Ca^{2+} and any extraframework tetrahedral aluminum oxide species present in the sodalite cages. These AlO_4 species have been observed both crystallographically and by ^{27}Al MAS NMR in CaA.[18] ^{27}Al MAS NMR of the CaY samples showed a resonance at 80 ppm that was assigned to the tetrahedral aluminum oxide in the sodalite cage. Although this resonance accounts for approximately 3−5% of the total aluminum intensity, the quadrupole coupling constant of species giving rise to the resonance is very small, in comparison to the framework aluminum nuclei, and hence the relative intensities of the two species need to be scaled appropriately,[20] resulting in a very small concentration of AlO_4 species in comparison to the aluminum in framework (less than 1 per unit cell). This is not sufficient to account for all the observed TRAPDOR effect.

No evidence for any significant Lewis acidity (due to aluminum Lewis acid sites) was detected for the samples prepared in an oven and with the vacuum line. This is in contrast to our earlier study of HY, where samples heated above 400 °C showed significant Lewis acidity.[6] The Lewis acidity created under these conditions results from the dehydroxylation of the Si−O(H)−Al linkage, and it may be that, under the conditions of temperature and vacuum required for this, the $CaOH^+$ and Si−O(H)−Al groups have already recombined to release water. The small amounts of water that are released at relatively elevated temperatures do not appear to result in a significant amount of steaming (and Lewis acidity), although they may help in the formation of the extraframework AlO_4 species. Interestingly, the sample of HY activated in an oven

does not show any Lewis acidity. This may be a consequence of the residual water that is present, which will coordinate or react with any Lewis acid sites that are created during the activation process. Finally, Brønsted acid-site protons are observed in CaY-600-oven which are rigidly held to the framework and do not appear to be in exchange with residual water molecules; these sites give rise to sizable $^{1}H/^{27}Al$ TRAPDOR effects even at room temperature. These Brønsted acid sites are unlikely to be located in the sodalite cages (where rapid exchange with the water is expected). It is these sites that are expected to be most reactive in the presence of the diarylalkenes.

^{1}H and ^{31}P MAS NMR clearly demonstrate the presence of high concentrations of Brønsted acid sites in CaY activated in an oven (≈2 per supercage, for activation at 500 °C). These presumably result from the following reaction:

$$Ca^{2+} + H_2O + Si{-}O{-}Al \rightarrow Ca(OH)^{+} + Si{-}O(H){-}Al$$

where Si−O−Al represents a portion of the zeolite framework. In contrast, samples carefully activated at 500−600 °C under vacuum contain negligible concentrations of Brønsted acid sites (<1 per unit cell). These quantitative conclusions are now used to help interpret the observations made in the reaction studies of the diarylethylenes.

The Brønsted acid sites appear to react stoichiometrically with the diaryl olefins sorbed in the oven activated CaY. Both diffuse reflectance spectral data (Figures 1 and 2 and Table 2) and mass-spectroscopy studies of deuterated CaY/solvents support the suggestion that the first step involves the protonation of the arylalkene to form a carbocation (e.g., **12**, Scheme 2). The absorptions at 428−486 nm that were observed with diffuse reflectance spectroscopy and that give rise to the intense colors of these zeolites could be assigned to this carbocation. In addition, use of a deuterated CaY lead to incorporation of deuterium at the C-2 position. Use of deuterated solvents for the diaryl sorption and product extraction gave 1,1-diphenylethane with a "D" in carbon-1. This indicates that the second hydrogen required to form the diarylalkane comes from the solvent.

Differences in behavior of CaY activated under different conditions, we believe, are the result of differences in the number of Brønsted acidic sites present in these structures. Furthermore, the reaction studies of **1a** performed as a function of loading level, which showed a slight reduction in product formation for a loading level of 2 per supercage is consistent with the numbers of Brønsted acid sites determined from NMR. Furthermore, this drop off with loading level, and for samples activated at different temperatures, is consistent with a stoichiometric reaction involving the Brønsted acid sites and not a catalytic reaction. The lower reactivity of the fluoro- and chloro-substituted arylalkenes is consistent with the formation of a carbocation as the first step of the reaction mechanism, the para-substituents on the aryl groups acting to destabilize the carbocation. Reactivity of the diaryl in other divalent-cation-exchanged zeolites was observed in the order CaY > SrY > MgY > BaY. This is presumably a consequence of the decreasing concentrations of Brønsted acid sites in these zeolites. The oxygen atoms in these zeolites may act as basic sites, basicity increasing for the alkaline-earth-exchanged zeolites with size of cation. Thus, the Brønsted acid sites in BaY may be expected to be the least acidic. However, the much smaller number of Brønsted acid sites that are expected for BaY, due to the larger Ba^{2+} cation, are likely to be a much more important contribution to the reduced reactivity. The lower reactivity for MgY may be due to the smaller Mg^{2+} cation. Although this should, in theory, favor the formation of $MgOH^{+}$, the smaller Mg^{2+} cation, located in the SII or SI′ positions, lies closer to the plane formed by the three coordinated oxygen atoms of the six rings than do the larger cations. Thus Mg^{2+} will be more effectively screened by these oxygen atoms. This may result in less effective polarization of any bound water molecules and, a consequently, less Brønsted acid sites. Thus, the number of Brønsted acid sites may be related to both cation size and cation location. NMR studies are, however, in progress to quantify the number of acid sites in these and a variety of other zeolites.

SCHEME 4: Brønsted Acid-Site-Mediated Geometric Isomerization of 1,2-Diarylethylenes

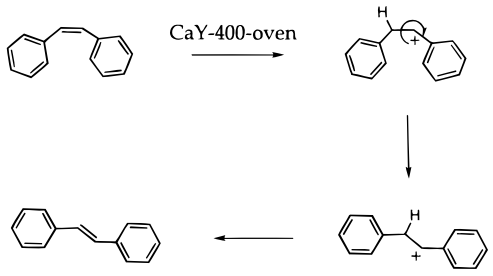

The proposed mechanism for the geometric isomerization of **11** within CaY-400-vacuum is shown in Scheme 4[4]. Again the reaction is initiated by protonation. Absence of reduction products suggests that either the cation generated by protonation does not survive long enough to abstract a hydride or the number of cations is not large enough to yield an appreciable amount of the reduction product. Given the negligible concentrations of Brønsted acid sites identified by ^{1}H and ^{31}P MAS NMR, we believe that it is the latter. Thus the final product (reduction or isomerization), appears to be controlled by the number of Brønsted acid sites present within CaY. When the number of Brønsted acid sites are large with respect to the number of olefin molecules present in a zeolite, the acid−base equilibrium favors the permanent formation of carbocations. These carbocations probably abstract a hydride ion from the solvent to yield the reduction products. When the number of Brønsted acid sites are relatively small, not enough carbocations are generated to yield significant amounts of reduction products. However under such conditions the acid sites can act as catalysts and effect an isomerization of an olefin from the thermodynamically less stable to the more stable isomer. This is similar to reactivity observed in NaY, where the low concentrations of Brønsted acid sites were observed to act catalytically, to cause rearrangements of a number of olefins.[21]

The reaction of the Brønsted acid site with the diaryl olefin results in a carbocation. This carbocation acts to provide charge neutrality with the framework. Subsequent reaction with the solvent must involve the extraction of hydride ion from the solvent, and a product or intermediate with a positive charge must be generated. One possibility is that recombination with the OH^{-} present as $CaOH^{+}$ may occur to maintain charge neutrality in the final set of products. This suggestion requires further experimental testing. At this stage, the source of the hydride, and the mechanism of the second addition, are still unclear.

At the moment, we are not certain of the structure of the species that is responsible for the long-wavelength absorption (>600 nm) observed in the diffuse reflectance studies. On the basis of the earlier studies of the behavior of vinylanisole and indene within CaY we speculate that a dimeric cationic species might be responsible for this absorption.[22] The dimeric cationic

SCHEME 5: Proposed Structures for the Persistent Carbocation Derived from Diphenylethylene

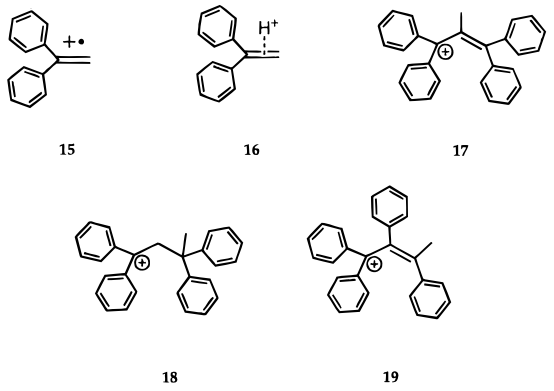

species may result from the reaction of a monomer cation with a neutral monomer to form a dimer cation (of unknown structure). This speculation is supported by the behavior of 1,2-diarylethylenes (**9** and **11**) which do not show an absorption at longer wavelengths. Only absorptions in the region of 300−370 nm were observed which were attributed to benzyl carbocations formed from the addition of a proton to **9** and **11**.[14] End capping of olefin should disfavor dimerization, especially within a confined space. This was also supported by the behavior of two terminal capped diarylethylenes **4** and **7** which only a gave a yellow color in the CaY-500-oven attributable to a monomer carbocation (Figure 4). In general these olefins gave the reduced products in low yields (Table 3).

A deep blue or green coloration of diphenylethylene in acidic media (in solution as well as on silica−alumina surfaces) has been reported previously.[23−28] In the past, several suggestions have been made for the coloration (Scheme 5). One proposal is that the color is due to a monomer radical cation (**15**, Scheme 5).[24] Unfortunately, the absorption spectrum for 1,1-diphenylethylene radical cation in solution has not been conclusively identified.[29] However, reported spectra, assigned to the 1,1-diphenylethylene radical cation, do not correspond with the spectrum reported in this or previous studies. Another suggestion for this colored species is an olefin−acid π-complex (**16**, Scheme 5).[23] Since the original proposal, this has not received much experimental support. Suggestions that the species may be a cation derived from a dimeric or a trimeric species have been made.[25−27] Two structures **17** and **18** (Scheme 5) have been proposed for the dimeric cation.[25a,27] While these are likely, formation of such structures would require rearrangements that are thermodynamically less favorable.[25a,27] We tentatively assign the structure responsible for the blue color to be **19**, and a proposed mechanism for its formation is shown in Scheme 6.

A key step in the reaction sequence outlined in Scheme 6 is the conversion of carbocation **18** to the carbocation **19**. This we believe occurs through a series of acid−base equilibria as illustrated in Scheme 6. The reaction sequence in Scheme 6 bears a close resemblance to the behavior of indene and vinylanisole published earlier.[1a,b] Olefin **20**, once formed via a proton-mediated dimerization process, can be protonated by the acidic sites present in CaY. Protonation can occur either at the terminal carbon leading to **18** or at the middle carbon yielding **21**. Of the two processes, the former is expected to be favored since it generates a more stable cation. However, the latter is also likely to take place, albeit in low yields, since this cation will also be stabilized by adjacent phenyl groups via formation of a nonclassical phenonium ion. Given the fact that the cation **21** will be stabilized by neighboring phenyl groups, direct conversion of **18** to **21**, via hydrogen migration, by passing the olefin **20** is also possible. Once **21** is formed, its transformation to **22** would be expected via a phenyl migration. Further reactions, as outlined in Scheme 6, would yield the carbocation **19**. We suggest that the blue species absorbing at 610 nm is the carbocation **19**. Of the various species suggested to be responsible for the 610 nm absorption (Scheme 5), the cationic species **17**, suggested by Rooney and Hathaway,[25a] and **19**, suggested in this report, bear close

SCHEME 6: Proposed Mechanism for the Formation of Persistent Carbocations 17 and 19

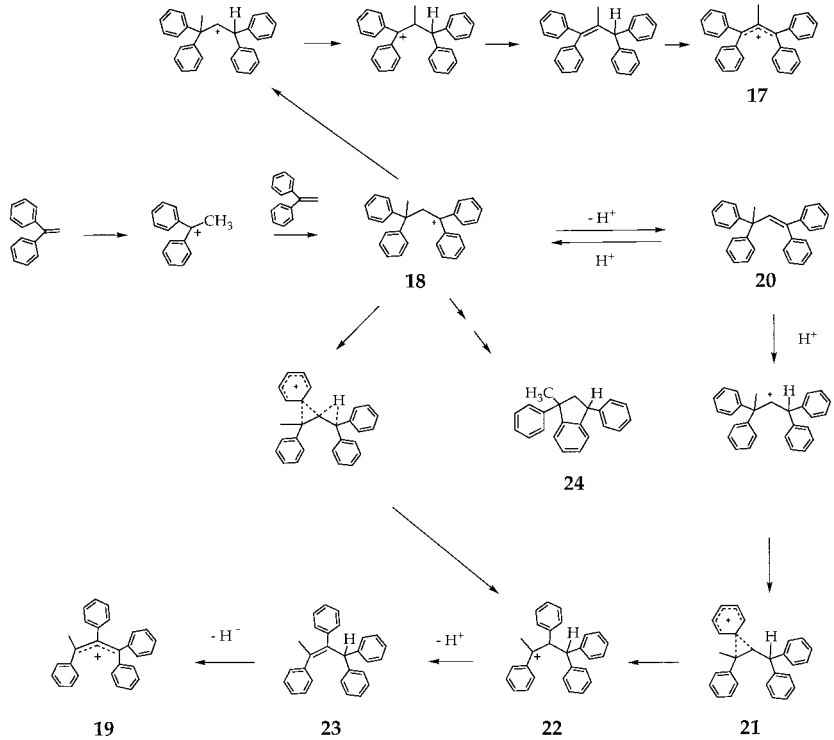

similarity. Structure **17** results from the migration of a "methyl" group while **19** comes from the migration of the phenyl group. As indicated in Scheme 6, migration of a phenyl group is more likely due to stabilization of the intermediate via phenonium ion formation.[30] Further work is underway to confirm the suggestion.[31]

Conclusions

Variable-temperature ^{1}H MAS NMR spectra of CaY, calcined in an oven, show resonances of Brønsted acid sites, Al−OH species, and Si−OH groups. A "Pake doublet" was also observed, with an isotropic chemical shift close to that of the Brønsted acid sites, resulting from proton−proton dipolar coupling between the two protons in a rigidly bound water molecule. This resonance is assigned to water bound to a calcium cation i.e., $Ca(OH_2)_n^{2+}$ ($n = 1$) in the sodalite cages. ^{1}H/^{27}Al TRAPDOR NMR demonstrated that the water molecules are in close proximity to aluminum atoms. The ^{1}H resonances from $CaOH^+$ groups in the sodalite cages resonate at 2.1−2.8 ppm and are most easily seen in the ^{1}H/^{27}Al TRAPDOR spectrum when ^{27}Al irradiation was applied. A concentration of approximately 16 Brønsted acid sites/unit cell was determined by adsorbing TMP molecules on the sample activated at 500 °C. Only a small number of Brønsted acid sites were detected, when samples were carefully calcined in a vacuum. No Lewis acidity was observed. A ^{1}H resonance at 0.7 ppm observed in the spectrum of CaY calcined at 200 °C is assigned to $CaOH^+$ groups in the supercages.

The number of Brønsted acid sites present within CaY is controlled by the mode of activation. This determines the activity of CaY and, in turn, the nature of the products obtained. For the reactions studies in this paper, the Brønsted acid sites reacted stoichiometrically when present in high concentrations, resulting in the reduction of the olefin. At lower concentrations, the Brønsted acid sites acted catalytically to affect isomerization reactions. Finally, this paper shows that a combined zeolite characterization and product reactivity study of the same materials, activated under identical conditions, can be very helpful in rationalizing the product distributions, especially in reactions where both a wide range of products are possible and with zeolites whose properties can vary significantly with activation conditions.

Acknowledgment. The National Science Foundation National Young Investigator program (Grant DMR-9458017) is thanked for their partial support of this research. The solid-state NMR spectrometer was purchased with a grant from the National Science Foundation (CHE-9405436). V.R. thanks the Division of Chemical Sciences, Office of Basic Energy Sciences, Office of Energy Research, U.S. Department of Energy, for support of this program.

References and Notes

(1) (a) Pitchumani, K.; Joy, A.; Prevost, N.; Ramamurthy, V. *J. Chem. Soc., Chem. Commun.* **1997**, 127. (b) Pitchumani, K.; Lakshminarasimhan, P. H.; Prevost, N.; Corbin, D. R.; Ramamurthy, V. *J. Chem. Soc., Chem. Commun.* **1997**, 181. (c) Pitchumani, K.; Lakshminarasimhan, P. H.; Turner, G.; Bakker, M. G.; Ramamurthy, V. *Tetrahedron Lett.* **1997**, 371. (d) Pitchumani, K.; Corbin, D. R.; Ramamurthy, V. *J. Am. Chem. Soc.* **1996**, *118*, 8152.

(2) Habgood, H. W, *J. Phys. Chem.* **1965**, *69*, 1764.

(3) Uytterhoeven, J. B.; Schoonheydt, R.; Liengme, B. V.; Hall, W. K. *J. Catal.* **1969**, *13*, 425.

(4) Ward, J. W. *J. Phys. Chem.* **1968**, *72*, 4211.

(5) Hunger, M.; Freude D.; Pfeifer, H.; Prager, D. *Chem. Phys. Lett.* **1989**, *63*, 221.

(6) Kao, H. M.; Grey, C. P. *J. Phys. Chem.* **1996**, *100*, 5105.

(7) Kao, H. M.; Grey, C. P. *Chem. Phys. Lett.* **1996**, *259*, 459.

(8) (a) Miale, J. N.; Chen, N. Y.; Weisz, P. B. *J. Catal.* **1966**, *6*, 278. (b) Venuto P. B.; Hamilton, L. A.; Landis, P. S. *J. Catal.* **1966**, *4*, 81.

(9) Costenoble, M. L.; Mortier, W. J.; Uytterhoeven, J. B. *J. Chem. Soc., Faraday Trans. I,* **1978**, *74*, 466.

(10) Costenoble, M. L.; Mortier, W. J.; Uytterhoeven, J. B. *J. Chem. Soc., Faraday Trans. I,* **1978**, *74*, 477.

(11) Yesinowski, J. P.; Eckert, H.; Rossman, G. R. *J. Am. Chem. Soc.* **1988**, *110*, 1367.

(12) Grey, C. P.; Vega, A. *J. Am. Chem. Soc.* **1995**, *117*, 8232.

(13) (a) McClelland, R. A.; Kangasabapathy, V. M.; Steenken, S. *J. Am. Chem. Soc*. **1988**, *110*, 6913. (b) Azarani, A.; Berinstain, A. B.; Johnston, L. J.; Kazanis, S. *J. Photochem. A: Chem*. **1991**, *57*, 175.

(14) McClelland, R. A.; Chan, C.; Cozens, F.; Modro, A.; Steenken, S. *Angew. Chem., Int. Ed. Engl.* **1991**, *30*, 1337.

(15) (a) Ward, J. W. In *Zeolite Chemistry and Catalysis*; Rabo, J. A., Ed.; American Chemical Society: Washington, DC, 1976; p 118. (b) Poutsma, M. L. In *Zeolite Chemistry and Catalysis*; Rabo, J. A., Ed.; American Chemical Society: Washington, DC, 1976; p 437.

(16) (a) Rothwell, W. P.; Chen, W.; Lunsford, J. H. *J. Am. Chem. Soc.* **1984**, *106*, 2452. (b) Lunsford, J. H.; Rothwell, W. P.; Shen, W. *J. Am. Chem. Soc.* **1985**, *107*, 1540.

(17) Rao, V. J.; Perlstein, D. L.; Robbins, R. J.; Lakshminarasimhan, P. H.; Kao, H.-M.; Grey, C. P.; Ramamurthy, V. *J. Chem. Soc., Chem. Commun.* **1998**, 269.

(18) (a) Corbin, D. R.; Farlee, R. D.; Stucky, G. D. *Inorg. Chem.* **1984**, *23*, 2922. (b) Pluth, J. F.; Smith, J. V. *J. Am Chem. Soc.* **1983**, *105*, 1192.

(19) Dempsey, E. *J. Phys. Chem.* **1969**, *73*, 3666.

(20) Massiot, D.; Bessada, C.; Coutures, J. P.; Taulelle, F. *J. Magn. Reson.* **1990**, *90*, 231.

(21) (a) Robbins, R.; Ramamurthy, V. *J. Chem. Soc., Chem. Commun.* **1997**, 1071. (b) Li, X.; Ramamurthy, V. *J. Am. Chem. Soc*. **1996**, *118*, 10666. (c) Robbins, R.; Crompton, E.; Ramamchandran, S.; Ramamurthy, V. Unpublished results.

(22) (a) Pitchumani, K.; Ramamurthy, V. *J. Chem. Soc., Chem. Commun.* **1996**, 2763. (b) Jayathirtha Rao, V.; Prevost, N.; Ramamurthy, V.; Kojima, M.; Johnston L. J. *J. Chem. Soc., Chem. Commun.* **1997**, 2209.

(23) For carbocation formation in solution: (a) Gold, V.; Hawes, B. W. V.; Tye, F. L. *J. Chem. Soc*. **1952**, 2167. (b) Gold, V.; Tye, F. L. *J. Chem. Soc*. **1952**, 2172. (c) Evans, A. G.; Jones, N.; Jones, P. M. S.; Thomas, J. H. *J. Chem. Soc*. **1956**, 2757. (d) Evans, A. G.; Jones, P. M. S.; Thomas, J. H. *J. Chem. Soc*. **1957**, 104. (e) Grace, J. A.; Symons, M. C. R. *J. Chem. Soc*. **1959**, 958.

(24) For carbocation formation on a silica−alumina surface, see the following: (a) Leftin, H. P.; Hall W. K. *J. Phys. Chem*. **1960**, *64*, 382. (b) Leftin, H. P. *J. Phys. Chem*. **1960**, *64*, 1714. (c) Leftin, H. P.; Hall, W. K. *J. Phys. Chem*. **1962**, *66*, 1457. (d) Leftin, H. P.; Hobson, M. C.; Leigh, J. S. *J. Phys. Chem*. **1962**, *66*, 1214. (e) Rooney, J. J.; Pink, R. C. *Trans. Farady Soc*. **1962**, 1632. (f) Hall, W. K. *J. Catal.* **1962**, *1*, 53.

(25) (a) Rooney, J. J.; Hathaway, B. J. *J. Catal.* **1964**, *3*, 447. (b) Dollish, F. R.; Hall, W. K. *J. Phys. Chem*. **1965**, *69*, 4402.

(26) Hirschler, A. *J. Catal.* **1963**, *2*, 428.

(27) Fornes, V.; Garcia, H.; Jovanvic, S.; Marti, V. *Tetrahedron* **1997**, *53*, 4715.

(28) Reviews: (a) Leftin, H. P.; Hobson, M. C. *Adv. Catal*. **1963**, *14*, 115. (b) Terenin, A. *Adv. Catal*. **1964**, *15*, 227.

(29) (a) Al-Ekabi, H.; Kawata, H.; de Mayo, P. *J. Org. Chem*. **1988**, *53*, 1471. (b) Shida; T.; Hamill, W. H. *J. Chem. Phys*. **1966**, *44*, 4372. (c) Brede, O.; Bos, J.; Helmstreet, W.; Mehnert, R. *Radiat. Phys. Chem*. **1982**, *19*, 1. (d) Mizuno, K.; Tamai, T.; Hashida, I.; Otsuji, Y.; Kuriyama, Y.; Tokumaru, K. *J. Org. Chem*. **1994**, *59*, 7329. (e) Konuma, S.; Aihara, S.; Kuriyama, Y.; Misawa, H.; Akaba, R.; Sakuragi, H.; Tokumaru, K. *Chem. Lett.* **1991**, 1897.

(30) (a) Bartlett, P. D., Ed. *Nonclassical Ions*; W. A. Benjamin: New York, 1965. (b) Pocker, Y. In *Molecular Rearrangements*; de Mayo, P., Ed.; Interscience: New York, 1963; Part 1, pp 1−25.

(31) At this stage, both **17** and **19** could account for the long λ absorption. Mechanism provided in Scheme 6 accounts for the formation of both **17** and **19** as well as for the isolated products **2**, **3**, **20**, and **24**.